



HAL
open science

Spatio-temporal analysis of a liquid jet using a sub-picosecond optical gate

S. Idlahcen, C. Rozé, L. Méès, T. Girasole, J. Blaisot

► **To cite this version:**

S. Idlahcen, C. Rozé, L. Méès, T. Girasole, J. Blaisot. Spatio-temporal analysis of a liquid jet using a sub-picosecond optical gate. 23rd Annual Conference on Liquid Atomization and Spray Systems, Sep 2010, Brno, Czech Republic. hal-02407468

HAL Id: hal-02407468

<https://hal.science/hal-02407468>

Submitted on 12 Dec 2019

HAL is a multi-disciplinary open access archive for the deposit and dissemination of scientific research documents, whether they are published or not. The documents may come from teaching and research institutions in France or abroad, or from public or private research centers.

L'archive ouverte pluridisciplinaire **HAL**, est destinée au dépôt et à la diffusion de documents scientifiques de niveau recherche, publiés ou non, émanant des établissements d'enseignement et de recherche français ou étrangers, des laboratoires publics ou privés.

Spatio-temporal analysis of a liquid jet using a sub-picosecond optical gate

S. Idlahcen^{*1}, C. Rozé¹, L. Méès², T. Girasole¹, J.B. Blaisot¹

¹UMR 6614-CORIA, CNRS, Université et INSA de Rouen
76801 Saint-Étienne du Rouvray Cedex, France

²CNRS, UMR 5509 LMFA, École centrale de Lyon
69134 Écully Cedex, France

Abstract

A Diesel jet visualization based on an ultra-short light pulse and a time-resolved detection is proposed. An optical gate, consisting of a BBO (Beta Barium Borate) crystal, allows to separate ballistic, refractive and scattered light. An imaging pulse passes through the studied medium while a gating pulse is used to open the gate. With this configuration, a spatial resolution of 10 μm and a temporal resolution of 270 fs are obtained. The gate duration is compatible with the typical dimensions of a liquid jet generated by a commercial automotive fuel injector. Preliminary results show that spatio-temporal diagrams of transmitted light through a spray may be acquired, showing clearly the separation between ballistic, refracted and scattered light.

Introduction

Optimal use of liquid fuel needs a perfect understanding of the liquid injection inside the combustion chamber and of its break-up into small droplets. High pressure injection leads to complex structures in the near field of the nozzle, where the liquid column is stripped of droplets, liquid filaments, etc. This highly non-homogeneous medium makes tough imagery due to the almost random propagation of light. Time resolved imaging techniques have been proposed [1,2,3,4,5] to visualise the liquid core in spite of the surrounding scattering droplets cloud. In first approximation, the light transmission through a strongly scattering medium consists of two components, a ballistic and a scattered one. The first peak corresponds to the ballistic photons which have not interacted with the scatterers and constitute the first detected light. Scattered photons undergo multiple interactions, their trajectories are elongated and they are time delayed by a few picoseconds (second peak). In time resolved imaging techniques (ballistic imaging), an appropriate temporal selection of the ballistic photons reduces the influence of the scattered photons. A shadowgraph of the liquid core is then obtained by limiting the scrambling effect of multiple scattering.

The efficiency of ballistic imaging has been demonstrated through a 3.5 mm-thick human breast tissue for a 8 ps time gate [6] and through a 5 mm spray with a 2 ps time gate [4]. The relation between the spray dimension and the appropriated time gate has not been clearly established from now, probably because it depends strongly on many parameters. However, scattered photons time delay clearly depends on the actual length of scattering medium. So, we can state that reducing the time resolution in ballistic imaging technique is suitable to investigate smaller sprays. Furthermore, a shorter time gate provides additional information on the liquid core, based on the separation between refractive light and ballistic light. Such a separation between scattering modes (reflection/diffraction, refraction, etc.) have been investigated experimentally [7] and numerically [8] in single scattering configurations and in a multiple scattering configuration [9].

Near the injector nozzle, the liquid has not yet completely exploded into a cloud of droplets. At this stage, the liquid keeps memory of the injector hole and is nearly cylindrical. Nevertheless, hydrodynamic surface instabilities appear in this domain and will lead to jet atomisation further from the nozzle. Some photons experience refractions through the liquid jet and may be delayed by a typical time $\Delta t = \frac{\Delta n d}{c}$, where Δn is the difference between the refractive index of the liquid and the surrounding gas, d is the diameter of the jet and c is the speed of light in free space. Knowing that in automotive internal combustion engines, diameter of injection hole is about 200 μm , a temporal detection with a resolution of about 300 fs is sufficient to discriminate refracted photons from ballistic ones. To reach this aim, an ultra-short light pulse (duration of 100 fs) illuminates the liquid jet and a time-resolved image is recorded thanks to an ultra-fast time gate and a single CCD camera.

No electronic device can achieve such an ultrafast detection and an optical gate must be used. Two kinds of optical gates may be found in the literature based on (i) an optical Kerr effect, or (ii) a second harmonic generation (SHG) in a non linear crystal. In the referenced papers, optical Kerr gate is obtained by inducing a temporary birefringence in a Kerr active liquid between two crossed polarisers [1,2,3,4,5]. The temporal resolution of the gate is fixed by molecular reorientation time of the Kerr liquid and is of the order of 1 ps or greater. The second kind of optical gate has been used to obtain ballistic images and detect hidden objects in a turbid medium

* Corresponding author: idlahcen@coria.fr

[10,11,12]. The aim of this paper is to study the potential of SHG crystal time gate to extract liquid shape properties of the liquid in the near field of an injector. In the next section, temporal and spatial resolutions are presented. Glass fibre and spray images are presented in the last section.

Experimental setup

The principle of optical gating is to divide the laser pulse of wavelength 800 nm into two pulses: the imaging pulse crosses the spray, while the gating pulse is used to open the time gate and may be shifted in time by means of a delay line. The time gate consists of a beta barium-borate (BBO) crystal, which has a quadratic nonlinearity. The imaging pulse and the gating pulse are incident on the crystal with an angle θ . First, collinear second harmonic generation (SHG) occurs, so that light at wavelength 400 nm is generated along the direction of each pulse. When the two pulses overlap spatially and temporally on the crystal, non-collinear second harmonic is generated in direction $\vec{k}(2\omega) = \vec{k}_1(\omega) + \vec{k}_2(\omega)$, which is the intermediate direction between the two collinear second-harmonic pulses. The crystal orientation is adjusted by a rotation around a vertical axis, in order to obtain the best conversion efficiency. The SHG is quasi-instantaneous, so that the gate duration is only limited by the gating pulse duration and angle between the pulses.

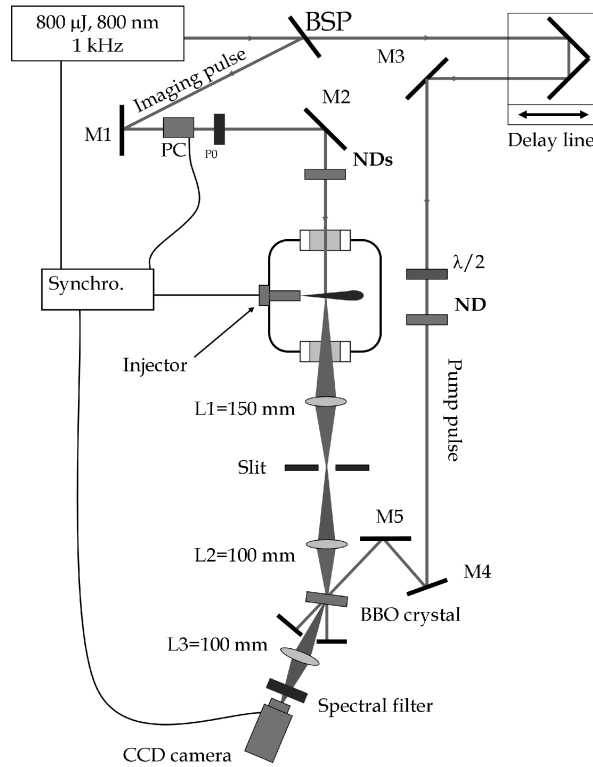


Figure 1. Schematic diagram of experiment

The integration of the gate inside the complete experimental setup is shown on Fig. 1. A Ti:Sa amplified laser system (800 nm, 1 kHz, 1 mJ) generates constant 100-femtosecond pulses. The beam profile is approximately Gaussian with a 5 mm full width at half maximum (FWHM). The laser pulse is separated in two parts by means of a beam splitter (BSP), the imaging pulse and the gating pulse. The gating pulse passes through a delay line, a half wave plate ($\lambda/2$) and a neutral density filter (ND), in order to adjust time delay, polarization direction and intensity. The imaging pulse passes through a Pockels cell (PC) in order to decrease the repetition rate of the pulses down to 1 Hz (the spray repetition rate). A set of neutral density filters (NDs) is then used to adjust the lighting power. The imaging pulse next illuminates the spray injected in a chamber, equipped with glass windows. Imaging pulse and gating pulse are incident on a BBO crystal with the angle θ between them. Careful optical alignments are conducted to overlap the two beams in both spatial and temporal domains on the crystal. Non-collinear second harmonic is generated at half angle $\theta/2$ between the directions of the two pulses direction when and where they overlap. A time gated second harmonic image of the spray is then formed by means of a lens (L1, $f=150$ mm). A vertical slit may be placed in the corresponding image plane, the use of which will be explained later. A second lens (L2, $f=100$ mm) forms a second image of the spray on the BBO crystal. A third lens is used to record the non collinear SHG on a CCD camera (Hamamatsu C9100). Light at fundamental

wavelength (800 nm) is scattered the camera. This noise source is eliminated by a spectral filter placed between the BBO crystal and the CCD camera, increasing notably the signal-to-noise ratio.

In order to measure the temporal profile of the gate, the power of the SHG pulse at angle $\theta/2$ is measured for various delays between the imaging pulse and the gating pulse, without liquid jet. The maximum corresponds to a temporal and spatial synchronisation between the two pulses in the BBO crystal, whereas the tails of the curve are obtained for nonzero delays between the pulses. The duration of the gate is defined as the full width at half maximum (FWHM) of the curve and is equal to 270 fs. It depends strongly on the angle θ between gating pulse and imaging pulse and finally, $\theta \approx 8^\circ$ seems to be a good compromise.

To evaluate the spatial resolution of the overall system, the image of an U.S. Air Force Chart is recorded on the camera. It allows of evaluate the modulation transfer function (MTF) of the gate for a range of spatial frequencies. This procedure has been used to assess the resolution of the imaging system to 10 μm .

Spatio-temporal analysis of the transmitted light

Images of a glass fibre

In order to investigate the potential of the BBO crystal based time gate, preliminary images have been recorded using a glass fibre as the object, without any other scattering medium. Fig. 2(a) shows the non-gated image of a fibre (diameter = 240 μm). The two strips located at each side of the image is the background light, whereas the thin line at the centre corresponds to refracted light into the fibre. When the optical gate is operating, the ballistic light may be isolated (Fig. 2(b)). By adjusting the delay line, refractive light is isolated (Fig. 2(c)). The time delay difference between images 2(b) and 2(c) is $\Delta\tau = 380$ fs, according to the fibre diameter $d=240$ μm and its refractive index $n \sim 1.5$.

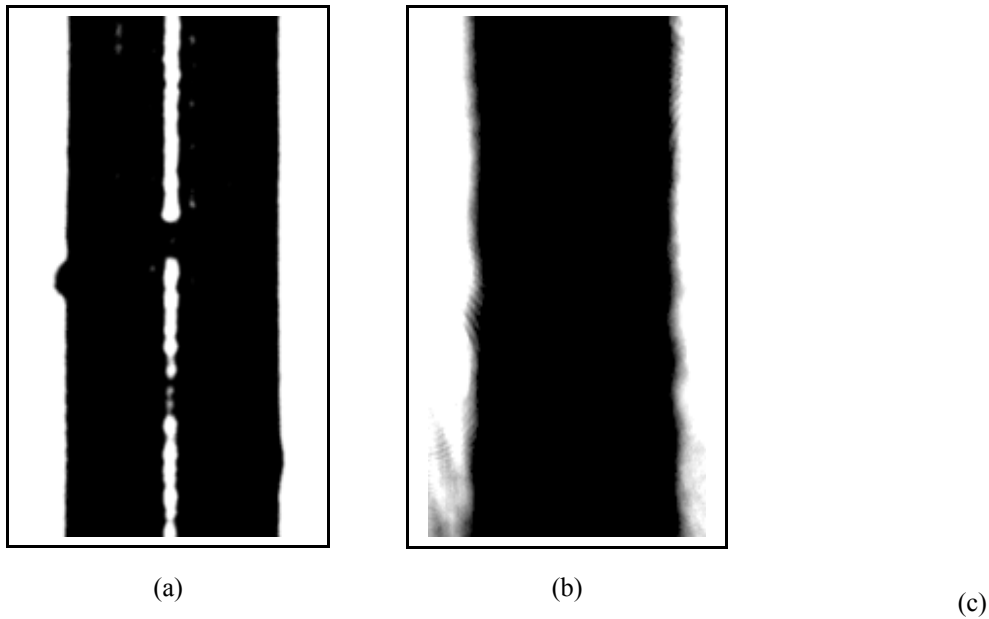


Figure 2. **a** Image of a fibre without optical gate **b, c** for two different delays of the optical gate

Images of the liquid jet near the injector

The same set-up has been applied to a Diesel jet visualisation. The injection pressure is 400 bars, the diameter of the nozzle hole is 200 μm and the liquid is injected at atmospheric pressure and ambient temperature in a chamber. In the near field of the injector, the liquid roughly keeps the cylindrical shape of the injector hole. Observation of refractive light is expected at this location. Time gated images are shown on Fig. 3, for two different delays between imaging and gating pulses. In both cases, the two pulses overlapped only partially, as a consequence of the angle θ , as schematically illustrated in the figure bottom. In figure 3(a), the delay line is adjusted in such a way that the gating pulse and the ballistic component of the imaging pulse overlap in the left side of the image. The right side of the image, where the two pulses do not overlap remains dark. In the middle part of the image, ballistic component does not overlap either temporally with the gating pulse. But refractive light, which is time delayed due to the jet crossing, overlap with the gating pulse and is clearly visible on the image. Conversely, when the delay is adjusted to overlap the gating pulse and ballistic light at the right side of the image, refracted light is no more detected and the liquid core appears to be completely dark (Fig. 3(b)). It must be noticed

that if the image and gating pulses are symbolised by rectangles on the schemas of Fig. 3, their temporal and spatial shapes are approximately Gaussian, so that the tails of the pulses may be used to detect light at time delays smaller than the 270 fs duration, depending on the sensitivity of the detector. The time delay between image 3(a) and 3(b) is $\Delta \tau = 500$ fs. Knowing the refractive index of the injected liquid equal to 1.46, we can deduce an estimation of the jet diameter of the jet diameter to about 325 μm .

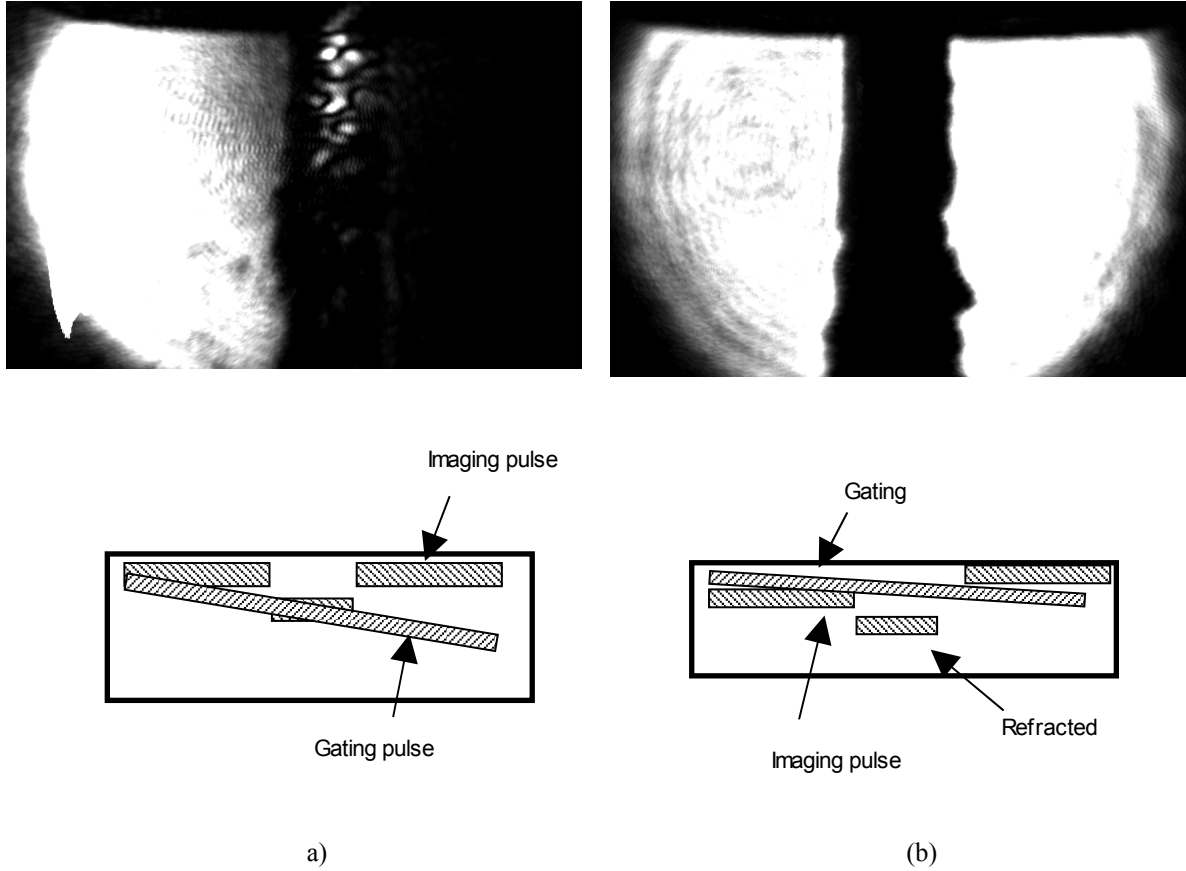


Figure 3. Images of the liquid jet at the exit from injector hole for two different delays between image and gating pulses

Spatio-temporal diagrams

The qualitative description of the preceding images leads to the conclusion that a spatio-temporal study of the light after interaction with an object is possible by changing the delay $\Delta \tau$ between the gating pulse and the image pulse. Indeed, the image on the camera is the result of the spatio-temporal correlation of the gating pulse with the image pulse along the width of the BBO crystal. The complete model is complex, because of interdependent phenomena: the spatio-temporal profile of each pulse, the angle between beams, the slight translation of one pulse relatively to the other inside the crystal due to their different propagation directions, etc. However, a rough interpretation of the image may be proposed by making some assumptions : (i) the image pulse and gating pulse are so short enough to be modelled by a time Dirac, (ii) the magnification of the optical system is large, so that the image pulse may be considered uniform in space before interaction with any object, (iii) the thickness of the BBO crystal is small, so that the shift of the gating pulse relatively to the image pulse is neglected, (iv) SHG light rays from the BBO are parallel.

With these assumptions, when the pump beam crosses the image beam somewhere in the crystal with angle θ between their propagation directions, a third pulse is produced, due to the SHG, at half angle. This intersection (point A on Fig. 4) produced a bright zone on the image recorded by the camera.

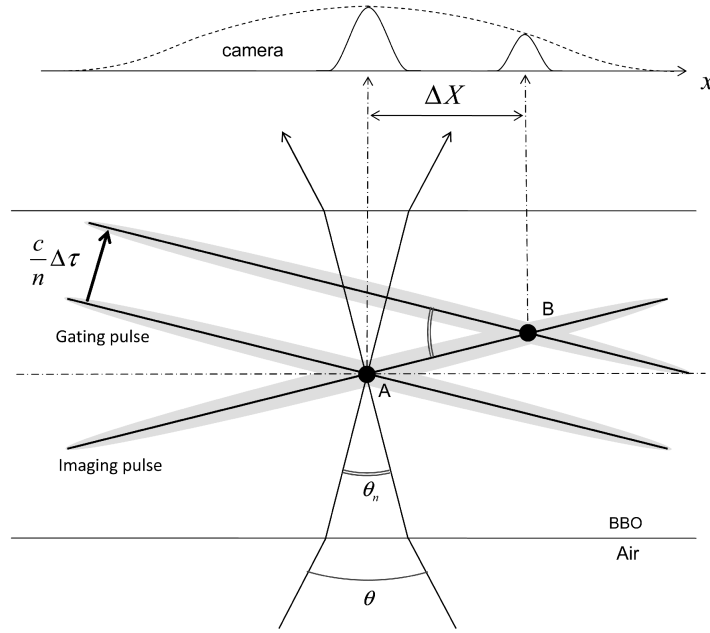


Figure 4. Relation between the maximum of intensity recorded on camera and the delay. The propagation directions of both pulses are in the horizontal plane

Now, if the gating pulse is affected by a delay $\Delta \tau$, the intersection point A is shifted to point B. Then a shift ΔX appears on the camera screen. Following the schema of Fig. 4, the relation between $\Delta \tau$ and ΔX leads to $\Delta \tau = \alpha \Delta X$, with $\alpha = 2 \frac{\sin \theta_n / 2}{c/n}$, where c is the speed of light in vacuum, θ_n is the angle between the two beams inside the crystal, and n the refractive index of BBO crystal.

The preceding considerations may then be applied to the fibre. Images are recorded by varying the delay $\Delta \tau$ between gating pulse and image pulse. For each value $\Delta \tau$, 20 images of size 1000x1000 pixels are recorded from the CCD camera and an average image $I(\Delta \tau, x, y)$ is computed. Then, intensity $I(\Delta \tau, x)$ is obtained by averaging the pixels of each column y . The spatio-temporal diagrams $I(\Delta \tau, x)$ are shown on Fig. 5, in two cases: (a) without the fibre and (b) with the fibre. In Fig. 5(a), the diagram is composed of ballistic photons. The bright area is oriented in accordance with the slope coefficient α previously introduced. The diagram of Fig. 5(b) shows a hole in the ballistic light, corresponding to the shadow of the fibre. As expected, refracted light undergoes a delay due to the fibre crossing. It shows that with a suitable processing, the interaction of light with an object may be followed in time with the time gate based on a BBO crystal.

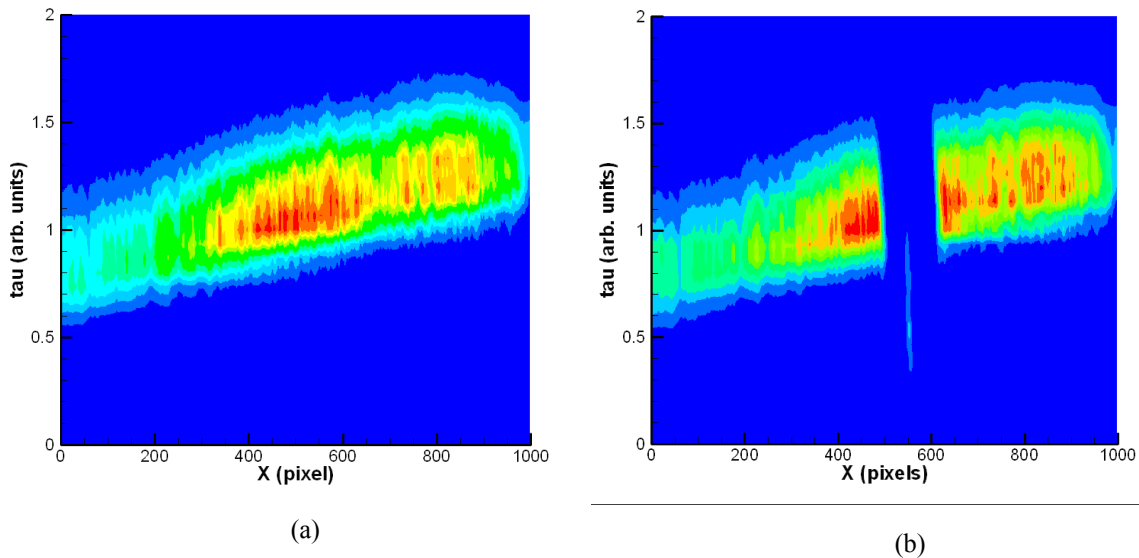


Figure 5. Spatio-temporal diagrams of the ballistic light: **a** without the fibre and **b** with the fibre

Spatio-temporal diagrams of the spray

The same process may be applied on the spray far from the nozzle. Fig. 6 is an example of a recorded image at 5 mm from the nozzle, showing many bright spots corresponding to scattered light, which do not exist in the case of the fibre. When the delay $\Delta\tau$ is changed, the texture of the image changes, leading to the conclusion that the source of this scattering may not be the same.

Again, images are recorded by varying the delay between the gating pulse and the image pulse. 100 images are recorded for each delay and the same image processing than for the fibre is applied. Spatio-temporal diagrams $I(\Delta\tau - \alpha \Delta x, x)$ are shown on Fig. 7 in two cases: (a) without the spray, in order to determine coefficient α , and (b) with the spray. Cases (c) and (d) show corrected diagrams by using a normalisation. One can observe that the optical gate is able to select the ballistic light. Nevertheless, due to the image averaging, and because of the limited dynamical range of the camera, neither scattered light nor ballistic one is visible on the spatio-temporal diagrams in the centre of the spray. Increasing the intensity of the imaging pulse is not a solution: a more intense imaging pulse would damage the camera. That is why a vertical slit has been added in an intermediate image plane, in order to eliminate the sides of the image (Fig. 1). The imaging pulse may then be more intense, without the risk of a camera damage. In this case, the intensity of the imaging pulse may be increased until getting a detectable level of the transmitted light through the spray.

We have used this method at 200 μm from the nozzle, in a more dense part of the spray. Images are again recorded by changing delay $\Delta\tau$ between gating pulse and imaging pulse. An average is made over 100 images for each $\Delta\tau$, and spatio-temporal diagrams are computed and shown on Fig. 8. Transmitted light at the centre of the spray is now observable. A time shift is visible between the reference diagram without spray (a) and the diagram with the spray (b). A delay of ~ 0.4 ps between the ballistic light and the transmitted light may be estimated by comparing these diagrams. It corresponds to an average jet liquid depth of about 300 μm , which is realistic at such distance of the nozzle.

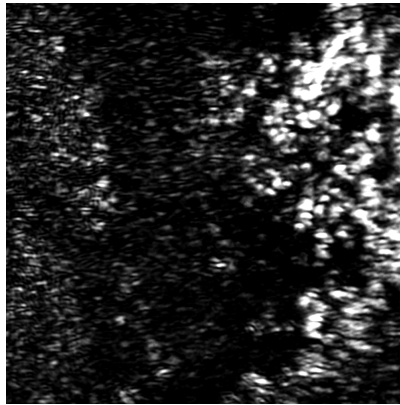
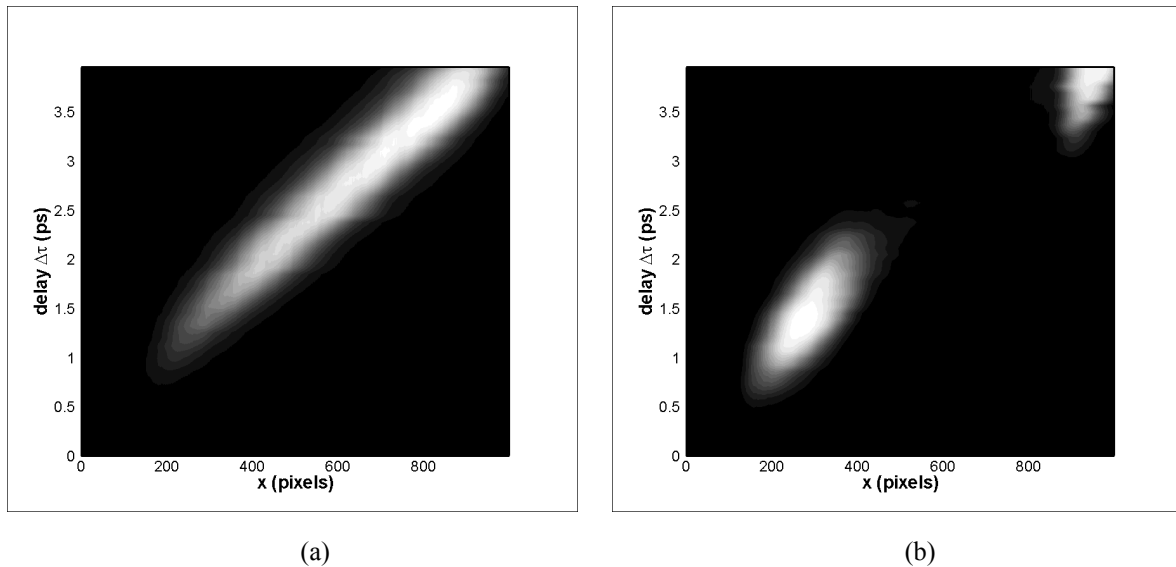


Figure 6. Image of the spray far from the nozzle, for some delays between gating pulse and image pulse



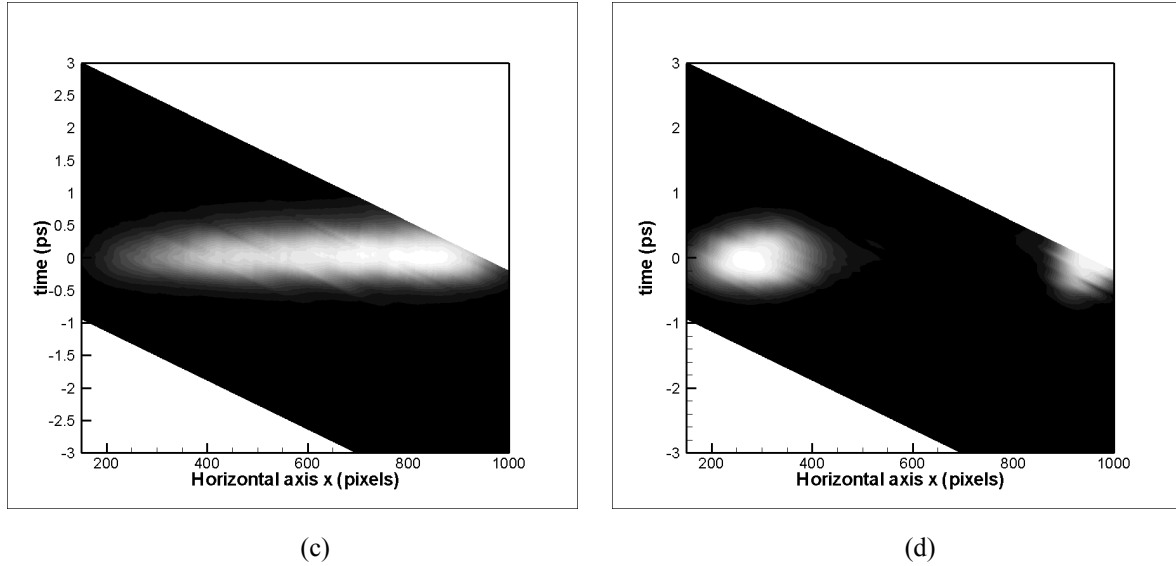


Figure 7. Spatio-temporal diagrams of light at 5 mm from the nozzle: **a** without spray, **b** which has interacted with the spray. Subfigures **c** and **d** are modified by normalisation

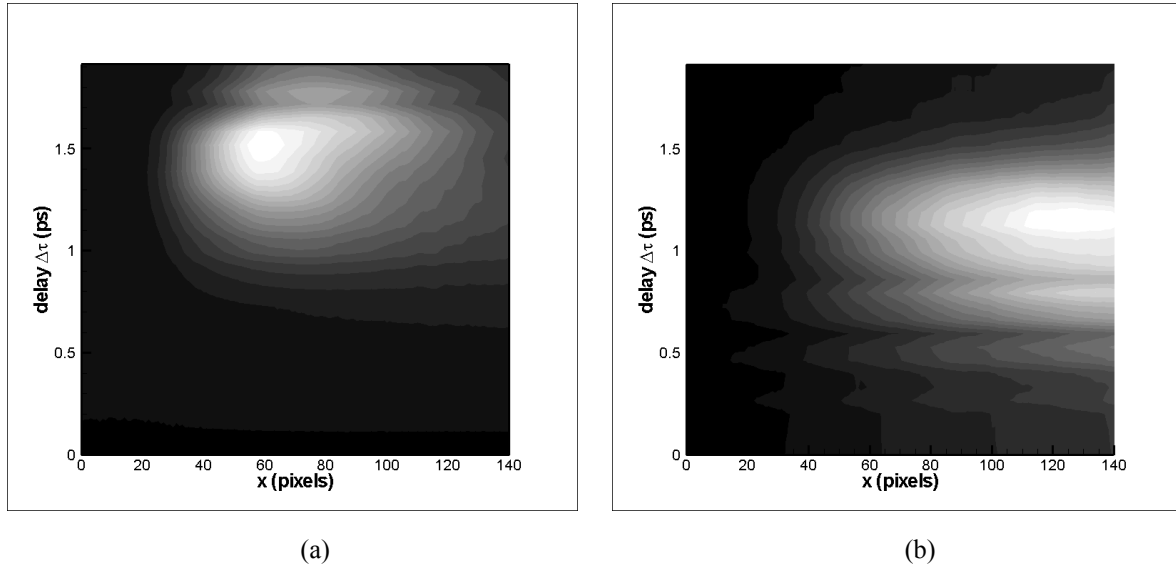


Figure 8. Spatio-temporal diagrams of transmitted light at 200 μm from the nozzle: **a** without spray, **b** with the spray

Conclusion

The use of an optical gate based on SHG in a BBO crystal allows to reduce the temporal resolution in ballistic imaging, which is now compatible with the dimension of the spray resulting from a Diesel injector. This duration opens the way to a new analysis of the liquid jet by studying the transmitted light as a function of time. In the near field of the nozzle, the time delay at which the refraction is observed is a measurement of the jet diameter. The refracted light pattern would be a signature of the surface state of the liquid. The first instabilities appearing in the liquid may then be quantified and compared for example with direct numerical simulations (DNS) [13] to evaluate if correct destabilisation mechanisms are taken into account in the simulations.

Spatio-temporal diagrams of transmitted light open perspectives to investigate liquid jet atomisation, including in high speed and high pressure conditions. The characterisation of the structure of the spray would be possible by the analysis of the image texture produced by the scattered light.

References

[1] Galland, P.A., Liang, X., Wang, L., Breisacher, K., Liou, L., Ho, P.P., and Alfano, R.R., *Proc. Am. Soc. Mech. Eng.* HTD-321:585-588 (1995).

- [2] Paciaroni, M., Hall, T., Delpanque, J.P., Parker, T., and Linne M., *Atomization and Sprays* 16:51-59 (2006).
- [3] Linne, M., Paciaroni, M., Halland, T., and Parker, T., *Exp Fluids* 40:836-846 (2006).
- [4] Schmidt, J.B., Schaefer, Z.D., Meyer, T.R., Roy, S., Danczyk, S.A., and Gord, J.R., *Appl Opt* 48:B137-B144 (2008).
- [5] Idlahcen, S., Méès, L., Rozé, C., Girasole, T., Blaisot, J.B., *J Opt Soc Am A* 26:1995-2004 (2009).
- [6] Wang, L., Ho, P.P., Liu, F., Zhang, G., and Alfano, R.R., *Science* 253:769-771 (1991).
- [7] Sbanski, O., Roman, V.E., Kiefer, W., and Popp, J., *J Opt Soc Am A* 17(2):313-319 (2000).
- [8] Méès, L., Gouesbet, G., and Gréhan, G., *Opt Comm* 194:59-65 (2001).
- [9] Calba, C., Rozé, C., Girasole, T., and Méès, L., *Opt Comm* 265:373-382 (2006).
- [10] Farsiu, S., Christofferson, J., Eriksson, B., Milanfar, P., Friedlander, B., Shakouri, A., and Nowak, R., *Appl Opt* 46(23):5805-5822 (2007).
- [11] Kuditcher, A., Hoover, B.G., Hehlen, M.P., Leith, E.N., Rand, S.C., and Shih, M.P., *Appl Opt* 40:45-51 (2000).
- [12] Abraham, E., Bordenave, E., Tsurumachi, N., Jonusauskas, G., Oberlé, J., Rullière, C., and Mito, A., *Opt Lett* 25:929-931 (2000).
- [13] Tanguy, S., Menard, T., and Berlemont, A., *J Comput Phys* 221(2):837-853 (2007).